Journal of Applied Polymer Science

Crystallization kinetics of thermoplastic elastomeric blends based on ground tyre rubber

Paulo S. Lima,[1] José M. Oliveira,[1,2] Vítor A. F. Costa[3]

[1]School of Design, Management and Production Technologies, University of Aveiro, Estrada do Cercal, 449, 3720-509 Santiago de Riba-Ul, Portugal

[2]CICECO, University of Aveiro, Campus Universitário de Santiago, 3810-193 Aveiro, Portugal

[3]Mechanical Engineering Department, University of Aveiro, Campus Universitário de Santiago, 3810-193 Aveiro, Portugal

Correspondence to: P. S. Lima (E-mail: plima@ua.pt)

ABSTRACT: This work analyzes the crystallization process of thermoplastic elastomeric blends (TPE) based on ground tyre rubber (GTR). More specifically it analyzes the effect of GTR and fresh rubber materials, like ethylene propylene diene monomer (EPDM) and ethylene propylene rubber (EPR), on the crystallization of binary and ternary polypropylene (PP)-based blends. The crystallization kinetics is studied under isothermal and nonisothermal conditions using differential scanning calorimetry (DSC). The kinetic parameters derived from the Avrami model are used to study the effect of temperature and rubber materials on the nucleation mechanism, the morphology of the crystalline structures, and the crystallization rate. Results reveal that GTR has a strong nucleating effect on PP and that its presence leads to higher crystallization rates. The EPDM presence has a slight effect on the PP crystallization process whereas EPR has no significant effect. From the DSC curves it is possible to detect an inverse relationship between temperature and the crystallization rate. © 2015 Wiley Periodicals, Inc. J. Appl. Polym. Sci. **2015**, *132*, 42589.

KEYWORDS: composites; crystallization; differential scanning calorimetry (DSC); kinetics; recycling

Received 10 February 2015; accepted 7 June 2015

DOI: 10.1002/app.42589

INTRODUCTION

End of life tyres (ELT) are a worldwide environmental problem. Specific mandatory regulations have been created to manage and deal ELT and several strategies are being pursued to promote a sustainable recovery, generally through the recycling of their materials or as energetic source.[1,2]

Ground tyre rubber (GTR), a by-product of ELT, has been used in several applications, like in sports fields and playground floors. The upcycle of this material through new added-value applications has led to the research of new thermoplastic elastomeric blends (TPE) based on GTR (TPE^{GTR}) and a polyolefin matrix. Because of the lack of adhesion between the polyolefin and GTR, chemical and physical strategies have been tried to enhance their compatibility such as regeneration or surface functionalization of the vulcanized GTR or the use of compatibilizing agents.[3–7]

A partial substitution of GTR by a fresh rubber material is another working strategy, with the advantage of improving the toughness behavior and simultaneously to act as a compatibilization agent between the materials. Ethylene propylene diene monomer (EPDM), ethylene propylene rubber (EPR), and styrene butadiene rubber (SBR) are usually chosen as fresh rubbers because of their chemical affinity with these materials. The ternary blends performance depends not only on the compatibility between the materials, but also on their structure, namely morphology and crystallinity. Several studies have already focused on the compatibility and morphology of these blends.[8–17] However, the GTR effect on the TPE^{GTR} blends crystallization kinetics still needs to be better understood and studied in more detail. The crystallization process of polymer blends is strongly affected by the nature of the blended materials. The presence of a particle or surface from another polymer in a semi-crystalline material may change a predominantly homogenous nucleation mechanism to a heterogeneous one, changing the crystalline structures and consequently the mechanical properties.[18,19] The processing conditions also have a considerable effect on the crystallization behavior. In injection molding, polymers are processed at high temperatures, pressures and shear rates and then cooled to the ejection temperature. For semi-crystalline polymers these processing conditions significantly affect the crystals nucleation and growth and consequently the spherulites number and size. A crystallization kinetics study is therefore of major relevance to predict the development of the crystalline

structures within the TPE^{GTR} blends, allowing to establish the most suitable injection molding conditions.[19–22]

The crystallization kinetics of polypropylene (PP)/EPDM and PP/EPR blends has been studied by several authors and the rubber effect on the PP crystallization process evaluated.[20,22–31] Usually, the rubber components affect the crystallization process, influencing the nucleation mechanism and, thereby, the nucleation density and growth of the spherulites. The rubber content, its molecular weight, and melt flow index (MFI) are some of the parameters that may contribute to hinder or induce the nucleation process. The resultant size and morphology of spherulites, as well as crystallinity, will have a strong effect on the blends mechanical behavior. In general spherulites of smaller sizes and perfection favor the toughness behavior of semicrystalline polymers and the yield stress and Young modulus are directly proportional to the crystallinity results.[24,32] Some authors analyzed the GTR effect on the crystallization process under nonisothermal conditions. Costa *et al.*[33] reported an increase on the crystallization temperature (T_c) with increasing GTR content on PP/EPDM/GTR blends. Wiessner *et al.*[34] analyzed noncompatibilized and peroxide compatibilized compounds of PP/GTR, and they concluded that GTR could have a nucleating effect on noncompatibilized PP/GTR blends and no effect on compatibilized blends. However, Silva *et al.*[35] indicated a T_c decrease with increasing GTR content for noncompatibilized and compatibilized PP/GTR blends, with maleic anhydride grafted polypropylene (PP-*g*-MA) as the compatibilization agent. The melting temperatures (T_m) also decrease with increasing GTR content. In low-density polyethylene (LDPE)/EPDM blends Costa *et al.*[36] detected a T_c continuous decrease with increasing EPDM and they also observed that an EPDM partial replacement by GTR on ternary blends leads to a stronger T_c reduction.

This work is part of an ongoing study that aims to contribute to a sustainable approach of GTR recycling through the development of TPE^{GTR} blends without the use of thermochemical methods.The mechanical properties of TPE^{GTR} blends based on PP, fresh rubbers and GTR have already been studied on previous works, with special focus on the compatibility between the materials and the morphology of the developed blends.[37,38] EPDM and EPR have been chosen as fresh rubber materials because of their toughness enhancement effect on PP-based blends and potential compatibility with GTR.

The main purpose of the present work is to study the crystallization kinetics of TPE^{GTR} blends under isothermal and nonisothermal conditions. The individual and combined effects of GTR and fresh rubbers on the PP crystallization process are analyzed using differential scanning calorimetry (DSC).

EXPERIMENTAL

Materials

The rubber materials used in this study are as follows: GTR from mechanical ground scrap tyres, FB 00–08, from Biosafe S.A., Portugal, obtained by an ambient grinding process, sieving class 635 to 20 mesh and density from 0.6 to 0.7 g/cm^3; an EDPM rubber, Buna® EP G2470 from Lanxess, with 68 wt % ethylene content, 4.2 wt % content of ethylidiene norbornene (ENB) as diene, 0.86 g/cm^3 density and a MFI of 0.5 g/10 min (230°C, 2.16 kg); and the EPR, Vistamaxx^{TM} 6202, from Exxon Mobile, with 15 wt % ethylene content, density of 0.86 g/cm^3 and a MFI of 26 g/10 min (230°C, 2.16 kg). A non-nucleated PP homopolymer, PPH10060 supplied by Total Petrochemical, suited for injection moulding of very thin and complex parts, was used as the thermoplastic material, having a MFI of 35 g/10 min (230°C, 2.16 kg) and density of 0.91 g/cm^3.

Blends Composition

An experimental procedure was established to evaluate the individual and combined effects of the rubber materials on the crystallization process of PP-based blends (Table I). A first set of binary blends, with varying weight content, were developed to study the individual effect of the rubber components: EPR, EPDM and GTR. A second set of ternary blends were formulated to study the effect of 30 wt % content replacement of fresh rubber material (EPDM or EPR) by GTR.

Melt Mixing and Samples Preparation

The blends formulation was made in a Brabender mixer type at 180°C and 60 rpm rotor speed. For the binary blends formulation the PP was placed in the mixer chamber and after a 2-min period the rubber components were added for an additional 8-min mixing time. The formulation of the ternary blends was performed in two stages to promote a better encapsulation of the GTR particles by the fresh rubber material, EPDM or EPR.[13] At the first stage the fresh rubber and GTR were mixed during 8 min and then milled to obtain the granules for the next blending stage. At the second stage, PP was placed in the mixer chamber during 2 min. The rubber mixtures prepared in the first phase were then added and mixed during an additional 8 min period.

For injection moulding purposes the blends were then milled into granules and a 65 tons Inauton D65 injection moulding machine was used to produce test specimens, with the following injection moulding parameters: 220°C injection temperature, 35 bar holding pressure and mould temperature of 40°C.

Phase Morphology. The implemented strategy for blends formulation led to promising results concerning the compatibilization of GTR with the polymer matrix. Figure 1 shows the morphology of TPE^{GTR} blends analyzed in previous works.[37,38] It is possible to verify some fibrillar type structures between the GTR particles and the polymeric matrix, an indication of compatibility between the materials.

Differential Scanning Calorimetry

The calorimetry experiments were run on Shimadzu DSC-60 equipment and carried out at isothermal and nonisothermal conditions.

Isothermal Experiments. The isothermal experiments were run at a scan rate of 10°C/min. Samples of about 10 mg were heated to 200°C for 10 min to eliminate previous thermal and mechanical history of the blends, and rapidly cooled to the crystallization temperature, (T_c) and maintained at that temperature during the time needed to complete the crystallization of PP, assessed by the endpoint of the exothermal peak in the DSC

Table I. Blends Nomenclature and Composition

Blends composition: PP (**P**); GTR (**G**) Rubber (**R**): EPDM (**E**) or EPR (**V**); $\mathbf{P_{x1}(R_{y1}G_{y2})_{x2}}$ (1) Constraints: $x1 + x2 = 100$						
	$y1 + y2 = 1$	Designation	PP (%wt)	EPDM (%wt)	EPR (%wt)	GTR (%wt)
Reference material:		P_{100}	100	0	0	0
Binary blends $\mathbf{P_{x1}(R_{y1}G_{y2})_{x2}}$ $x_1 = (70;50;30)$ $y_1 = (0; 1)$	**R=EPDM (E)** with: $y2=0$	$P_{70}E_{30}$	70	30	0	0
		$P_{50}E_{50}$	50	50	0	0
		$P_{30}E_{70}$	30	70	0	0
	R=EPR (V) with: $y2=0$	$P_{70}V_{30}$	70	0	30	0
		$P_{50}V_{50}$	50	0	50	0
		$P_{30}V_{70}$	30	0	70	0
	$P_{x1}G_{x2y2}$ with: $x1=70$ and $y1=0$	$P_{70}G_{30}$	70	0	0	30
Ternary blends	**R=EPDM (E)**	$P_{70}(E_{0.7}G_{0.3})_{30}$	70	21	0	9
$\mathbf{P_{x1}(R_{y1}G_{y2})_{x2}}$ $x_1 = (70; 50; 30)$ $y_1 = 0.7$	**R=EPR (V)**	$P_{50}(E_{0.7}G_{0.3})_{50}$	50	35	0	15
		$P_{30}(E_{0.7}G_{0.3})_{70}$	30	49	0	21
		$P_{70}(V_{0.7}G_{0.3})_{30}$	70	0	21	9
		$P_{50}(V_{0.7}G_{0.3})_{50}$	50	0	35	15
		$P_{30}(V_{0.7}G_{0.3})_{70}$	30	0	49	21

curve. Different crystallization temperatures were analyzed on a range between 117°C and 129°C (Table II). Heat generated during the isothermal crystallization, ΔH_c, was recorded as a function of time and the degree of crystallization (X_c) obtained integrating the area under the crystallization peak, accordingly to the following equation:

$$X_c(t) = \frac{\Delta H(t)}{\Delta H_0} \quad (1)$$

where $\Delta H(t)$ is the heat released during the crystallization process [J/g] and ΔH_0 the melting heat of a perfect PP crystal, taken as 207 J/g.[39]

The relative degree of crystallization, $X_r(t)$, was determined as:

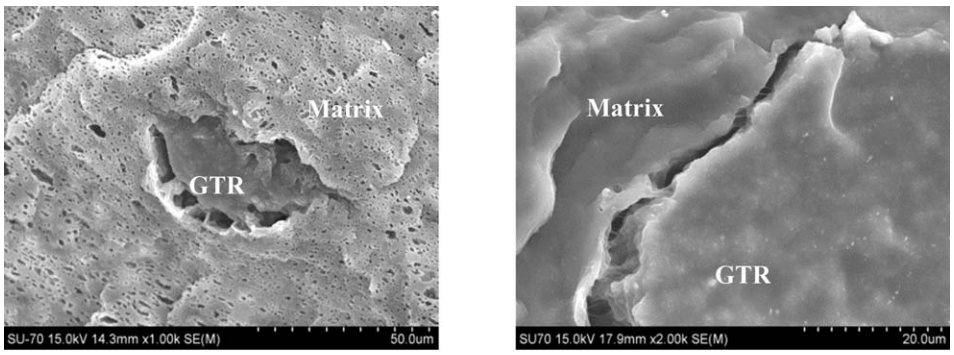

a) $P_{50}(E_{0.7}G_{0.3})_{50}$ blend. b) $P_{50}(V_{0.7}G_{0.3})_{50}$ blend.

Figure 1. SEM micrographs of $P_{50}(E_{y1}G_{y2})_{50}$ blends, etched with xylene (15 min, 50°C).

Table II. Blends Crystallization Parameters

Blend	T_c (°C)	$\tau_{1/2}$ (min)	Avrami parameters	
			k	n
P_{100}	123	2.35	0.087	2.27
	124	2.75	0.064	2.22
	125	3.58	0.041	2.15
	126	4.33	0.025	2.18
	127	5.65	0.018	2.06
$P_{70}G_{30}$	124	0.92	0.824	2.36
	125	1.29	0.347	2.74
	126	1.67	0.129	2.93
	127	2.45	0.045	2.94
$P_{70}E_{30}$	127	1.46	0.281	2.50
	128	1.85	0.162	2.56
	129	2.26	0.079	2.67
	130	3.29	0.038	2.84
$P_{50}E_{50}$	127	1.93	0.091	3.04
	128	2.40	0.060	2.85
	129	2.97	0.029	2.91
	130	3.60	0.024	2.66
$P_{30}E_{70}$	120	2.73	0.174	2.36
	121	2.15	0.106	2.31
	122	2.31	0.058	2.64
	123	2.91	0.046	2.48
$P_{70}V_{30}$	123	2.70	0.070	2.27
	124	3.23	0.042	2.32
	125	3.57	0.032	2.37
	126	4.55	0.018	2.37
$P_{50}V_{50}$	121	1.99	0.128	2.32
	122	2.36	0.090	2.30
	123	2.97	0.086	2.18
	124	3.10	0.049	2.28
$P_{30}V_{70}$	117	1.95	0.138	2.30
	118	2.30	0.089	2.31
	119	3.11	0.032	2.59
	120	4.19	0.038	2.18
$P_{70}(E_{0.7}G_{0.3})_{30}$	126	1.42	0.241	2.65
	127	2.08	0.087	2.85
	128	2.91	0.035	2.77
	129	4.53	0.005	3.26
$P_{50}(E_{0.7}G_{0.3})_{50}$	126	1.40	0.254	2.59
	127	1.94	0.091	2.89
	128	2.68	0.033	2.94
	129	4.58	0.009	3.01
$P_{30}(E_{0.7}G_{0.3})_{70}$	125	1.01	0.565	2.27
	126	1.63	0.193	2.29
	127	2.21	0.066	2.83
	128	3.67	0.021	2.67
$P_{70}(V_{0.7}G_{0.3})_{30}$	126	1.29	0.303	2.76
	127	1.83	0.102	3.02
	128	3.30	0.014	3.28
	129	5.95	0.005	2.90
$P_{50}(V_{0.7}G_{0.3})_{50}$	126	1.32	0.289	2.62
	127	1.83	0.087	3.09
	128	3.10	0.018	3.19
	129	5.41	0.008	2.81
$P_{30}(V_{0.7}G_{0.3})_{70}$	125	1.17	0.442	2.22
	126	2.51	0.187	2.89
	127	2.74	0.045	3.15
	128	3.76	0.010	3.22

$$X_r(t) = X_c(t)\frac{\Delta H_0}{\Delta H_T} = \frac{\int_0^t (dH/dt)dt}{\int_0^\infty (dH/dt)dt} \quad (2)$$

where ΔH_T is the total heat released during the crystallization process [J/g].

The blends crystallization kinetics were analyzed on the basis of the Avrami model, eq. (3), used to describe the development of the relative degree of crystallization (X_r) on isothermal processes.[40] The kinetic parameters n and k are used to deduce the nucleation mechanism, morphology and also the overall crystallization rate of PP:

$$X_r(t) = 1 - e^{-kt^n} \quad (3)$$

The Avrami exponent n is used to deduce the crystal growth mechanisms. The integer values of n will depend on the nucleation mechanism, homogeneous or heterogeneous, and on the type of crystal growth, one-dimensional (rods), two-dimensional (discs), or three-dimensional (spheres). The rate constant k is related with the crystal growth and nucleation rates.[41–44]

The kinetic parameters can be determined from the logarithmic form of the Avrami model, equation (4), through the plot of $\log[-\ln(1 - X_r)]$ versus $\log t$. The Avrami exponent n corresponds to the slope of the represented curve and $\log k$ to its intercept.

$$\log[-\ln(1-X_r)] = \log k + n \log t \quad (4)$$

Nonisothermal Experiments. The nonisothermal experiments were run at a scan rate of 20°C/min using samples of about 10 mg. Two heating cycles were performed with a temperature range between −120°C and 200°C. In the first cycle the samples were heated to 200°C and held for one minute at this temperature to eliminate the influence of thermal and mechanical history. Then they were cooled with nitrogen gas to −120°C and heated again to 200°C. The melting and crystallization

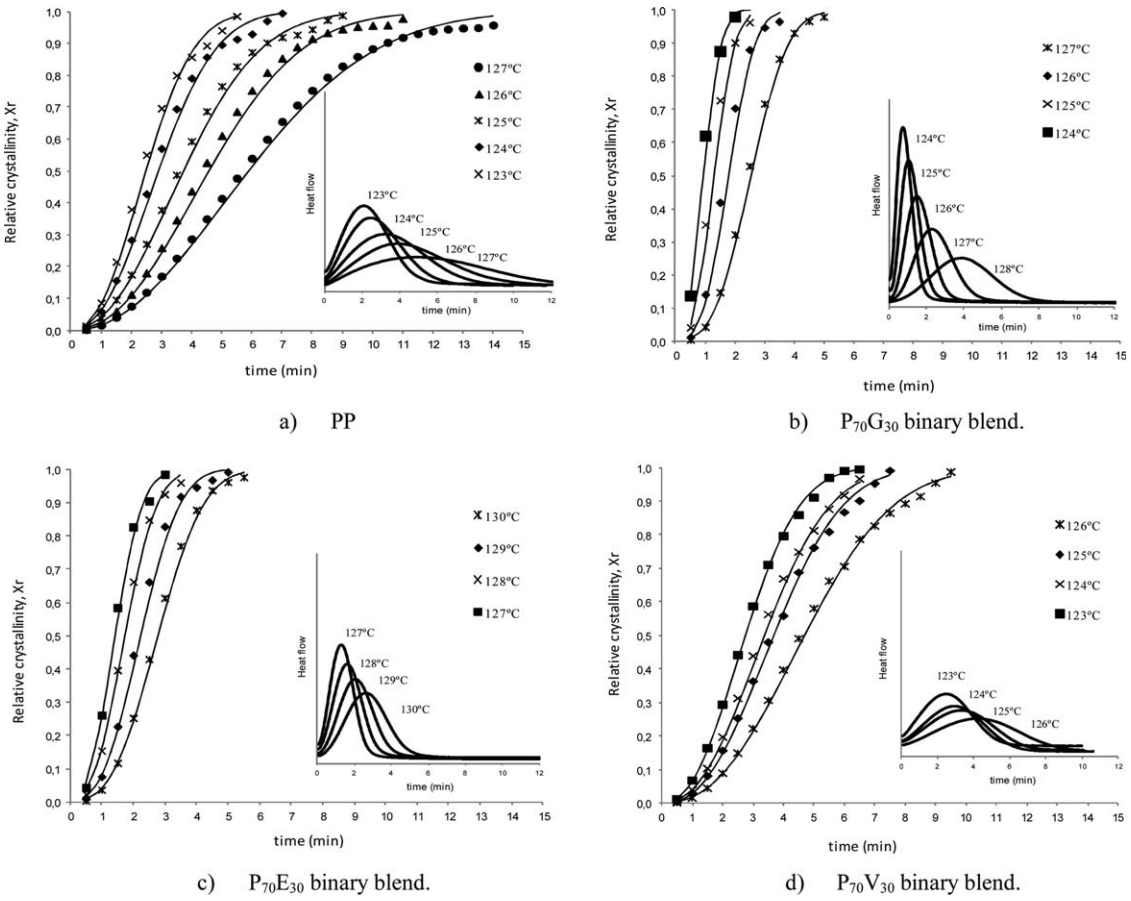

Figure 2. DSC curves and relative degree of crystallinity (X_r) as function of time, for PP and for some of the binary blends.

temperatures were recorded during the second heating scan. The melting enthalpy (ΔH_m) and crystallization enthalpy (ΔH_c) were calculated under the area of the melting and crystallization peaks, respectively, and the crystallinity (X_c) was obtained from the relationship:

$$X_c(\%) = \frac{\Delta H_m}{\Delta H_0} \times 100 \quad (5)$$

For comparative purposes the crystallinity results must take in consideration the blend PP weight content, which can be done using the following relationship:

$$\text{Corrected crystallinity: } X_c^c(\%) = \frac{\Delta H_m}{(1-\phi)\Delta H_0} \times 100 \quad (6)$$

ϕ is the weight fraction of rubber in the blend.

Optical Microscopy

Reflected-light microscopy observations were carried out on a Nikon Eclipse L150 microscope. The samples were melted for 2 min in a hot plate and the crystallites morphology examined upon cooling.

RESULTS AND DISCUSSION

Isothermal Crystallization

DSC curves and the relative degree of crystallinity (Xr) are plotted as function of time in Figure 2. The T_C interval under which the isothermal analyses were run was found to be dependent of the blends composition, particularly for the binary blends with higher rubber content. The Avrami parameters n and k are quite similar (Table II), indicating similar crystallization processes occurring at different temperature ranges. Kang *et al.*[45] also reported this behavior when studying the crystallization of isotactic PP polymerized with different Ziegler–Natta catalysts, suggesting that the isothermal T_c interval should be adequately selected in isothermal analysis.

The crystallization time increases with increasing T_c for all the analyzed blends, which shows a reduction of the overall crystallization rate with increasing temperature. A decrease on supercooling and lower nucleation and growth rate with increasing crystallization temperature agrees with crystallization kinetic theory.[45,46]

From the DSC curves crystallization rate can be estimated by determining the period to achieve 50% crystallization, half time crystallization ($\tau_{1/2}$), calculated from the onset and endset of crystallization (Table II). Higher $\tau_{1/2}$ values imply a slower crystallization process. Regarding PP as reference the $\tau_{1/2}$ decreases significantly for the $P_{70}G_{30}$ blend, slightly decreases for the $P_{70}E_{30}$ blend and similar result was found for the $P_{70}V_{30}$ blend. These results show the GTR presence leads to the highest crystallization rate, revealing its strong nucleating effect in PP. The EPDM presence has slight effect in the PP crystallization process whereas EPR has no significant effect. This result also reveals

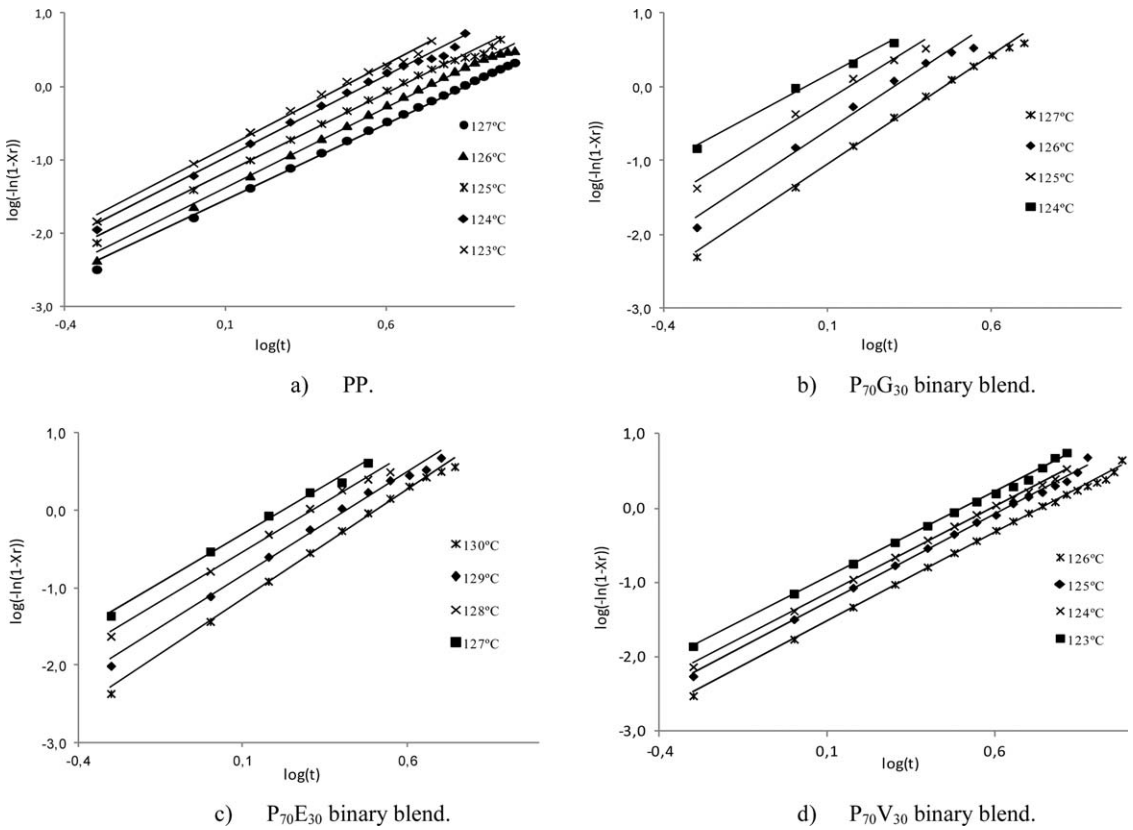

Figure 3. The logarithmic form of the Avrami model [eq. (4)].

the effect of the EPDM content on the PP crystallization. A smaller decrease of $\tau_{1/2}$ with increasing EPDM content suggests that above certain limits of the rubber phase can have an impingement effect on the spherulitic growth.

Results obtained from the Avrami model (Figure 3) show an increase of the rate constant k with the decrease of the crystallization temperature (Table II).

Analysing the k parameter for the 70/30 binary blends different effects of the rubber materials on the crystal growth rate and nucleation density can be found. The GTR presence leads to significant increase of k showing to have the highest effect of the rubber materials on the crystallization process. EPDM leads to a smaller k increase, whereas EPR leads to no significant changes in k. The same relationship between the EPDM content and the spherulitic growth (seen from the $\tau_{1/2}$ results) can be verified on the k results. A *k* increase for the $P_{70}E_{30}$ blend and reduction for the $P_{50}E_{50}$ and $P_{30}E_{70}$ blends suggest that above certain contents of the EPDM starts to constrain the spherulitic growth.[45]

Based on the Avrami exponent *n*, the rubber materials effect on the nucleation and morphology can be analyzed. The Avrami exponent *n* varies between 2 and 3. The noninteger values may be explained by a mismatch between some of the polymer characteristics and the Avrami equation simplification, such as the existence of secondary crystallization process, mixed nucleation modes, changes on the material density, and also by some experimental factors.[44,47] The increase of the Avrami exponent is consistent with changes from predominantly homogeneous mechanism in PP to a heterogeneous mode.

The EPDM presence induces a small increase of *n* while EPR has no apparent effect, which indicates that the EPR copolymer does not affect the overall morphology of the crystalline structures. The Avrami exponents closer to 2 may imply the growth of two-dimensional disc-like superstructures, or the incomplete development of three-dimensional spherulites, leading to some sheaf-like intermediate morphology.[44,48] GTR has stronger effect on the crystallites microstructure. Avrami exponents closer to 3 suggest a heterogeneous nucleation mechanism followed by diffusion controlled spherulitic crystalline growth.[22,49,50] This effect of GTR can be seen in the ternary blends, particularly the blends with EPR. An increase of *Tc* with the incorporation of GTR in the EPR-based blends also indicates a nucleating effect of GTR.

Nonisothermal Crystallization

The DSC reference curves for PP, EPDM, and EPR materials and the 70/30 binary blends are shown in Figure 4. The PP homopolymer used as reference shows a melting temperature of 165.5°C and 47% crystallinity.

Melting Behavior. The melting curve obtained by DSC analysis gives us information about the crystallites melting process. Changes on the shape and position of the melting peaks are associated with the nature of the crystallites created during the cooling stage. The melting temperatures and melting enthalpies (Table III) were measured under the area of the melting peak.[36]

The rubber effect on the PP corrected crystallinity (X^c_c) was analyzed. For the P_{70} binary blends GTR induces the highest effect, leading to a 27% increase. The crystallinity of the PP

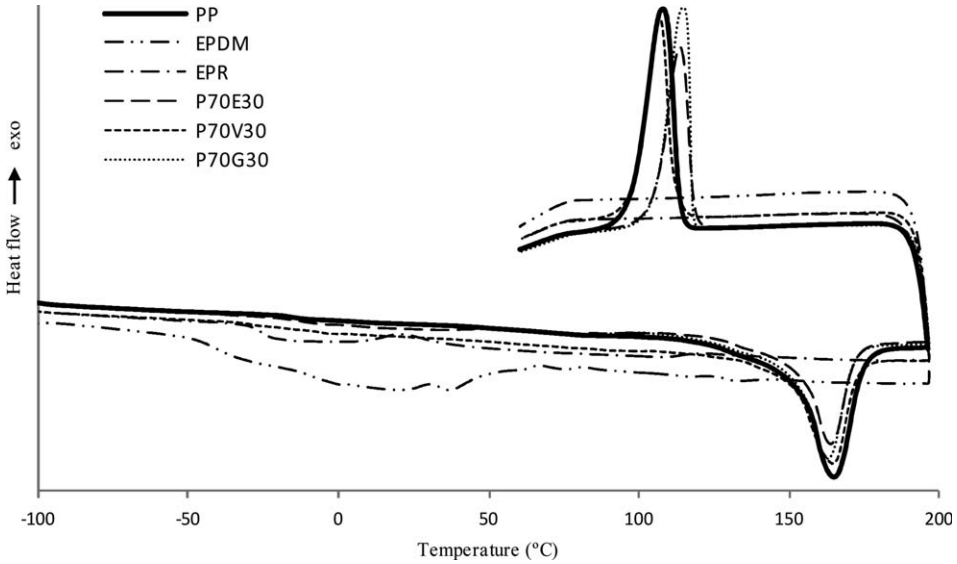

Figure 4. DSC reference curves.

component did not change significantly with fresh rubber presence: EPDM has a slight increasing effect and EPR the opposite result. The replacement of EPR or EPDM by GTR on the TPE^{GTR} blends leads to a higher crystallinity. This reflects the GTR effect detected on the binary blend.

The melting peaks show that PP has the highest T_m and also a wide melting peak, measured at its mid-height ($T_{me} - T_{mo}$). This reveals the presence of crystallites of higher lamellar thickness and perfection, as well the existence of greater morphological diversity and lamellar thickness distribution.[46] Rubber materials in PP blends lead to slight decrease of T_m which is an indication of morphological changes, such as imperfections in the crystallites or smaller lamellar thickness. For the same PP content in the binary blend, GTR has more significant effect on T_m than EPDM or EPR. All the analyzed blends show reduction of the melting peak width. This narrowing of the melting region is usually associated to lower dispersion of the crystallites geometry.[46] These changes in the melting peak can be related to a rubber hindering effect in the PP spherulite growth. Probably because of an entanglement effect of the rubber molecular chains into inter- and intraspherulitic regions, inhibiting the formation of the less perfect crystallites.[51,52] GTR can also interfere with the crystallites growth process, leading to smaller dimensional dispersion.

Crystallization Behavior. The crystallization curve obtained by DSC analysis gives us information about the crystallization process. Changes in the shape and position of the crystallization

Table III. DSC Melting Parameters

Blend	Melting peak temperature T_m (°C)	Onset melting temperature T_{mo} (°C)	Endset melting temperature T_{me} (°C)	Melting enthalpy ΔH_m (J/g)	Crystallinity X_c (%)	Crystallinity X_c^c (%) (corrected)
P_{100}	165.5	152.3	175.1	98.1	47.0	47.0
$P_{70}E_{30}$	163.9	154.8	171.7	73.9	35.3	47.9
$P_{50}E_{50}$	164.0	153.4	173.3	52.3	25.0	50.0
$P_{30}E_{70}$	164.0	152.5	172.8	30.4	14.6	48.5
$P_{70}G_{30}$	162.9	153.4	171.2	87.6	41.9	59.9
$P_{70}(E_{0.7}G_{0.3})_{30}$	164.5	152.4	174.9	76.4	36.6	52.2
$P_{50}(E_{0.7}G_{0.3})_{50}$	162.6	154.6	170.5	55.0	26.3	52.6
$P_{30}(E_{0.7}G_{0.3})_{70}$	164.0	153.3	173.1	33.2	15.9	52.9
$P_{70}V_{30}$	164.2	152.2	171.9	66.3	31.7	45.3
$P_{50}V_{50}$	163.4	151.3	170.9	48.9	23.4	46.8
$P_{30}V_{70}$	164.0	152.6	171.5	31.3	15.5	48.0
$P_{70}(V_{0.7}G_{0.3})_{30}$	163.9	152.0	173.0	69.5	33.3	47.6
$P_{50}(V_{0.7}G_{0.3})_{50}$	163.2	151.6	171.4	56.0	26.8	53.6
$P_{30}(V_{0.7}G_{0.3})_{70}$	162.5	152.0	170.9	35.1	16.8	55.9

Table IV. Blends Crystallization Parameters Obtained by DSC

Blend	Crystallization peak temperature T_c (°C)	Onset crystallization temperature T_{co} (°C)	Endset crystallization temperature T_{ce} (°C)	$T_{co}-T_c$	Nucleation rate I	Crystallization enthalpy ΔH_c (J/g)
P_{100}	108.1	114.5	98.0	6.5	6.8	107.6
$P_{70}E_{30}$	113.5	118.5	105.1	5.1	6.5	72.4
$P_{50}E_{50}$	110.7	116.2	101.1	5.5	4.0	57.1
$P_{30}E_{70}$	104.8	110.1	96.2	5.2	1.8	27.6
$P_{70}G_{30}$	114.7	117.9	105.7	3.2	16.2	83.9
$P_{70}(E_{0.7}G_{0.3})_{30}$	113.7	117.6	102.9	3.9	9.9	79.5
$P_{50}(E_{0.7}G_{0.3})_{50}$	114.3	117.8	105.9	3.5	8.3	59.4
$P_{30}(E_{0.7}G_{0.3})_{70}$	110.8	116.3	101.4	5.5	2.6	33.8
$P_{70}V_{30}$	106.5	111.6	98.3	5.1	6.6	79.4
$P_{50}V_{50}$	105.6	110.5	97.9	4.9	4.8	57.2
$P_{30}V_{70}$	96.7	103.8	88.0	7.1	3.5	37.8
$P_{70}(V_{0.7}G_{0.3})_{30}$	113.1	116.5	103.6	3.4	15.9	83.1
$P_{50}(V_{0.7}G_{0.3})_{50}$	112.9	116.3	104.2	3.3	10.5	64.1
$P_{30}(V_{0.7}G_{0.3})_{70}$	111.3	115.5	102.9	4.2	5.5	39.7

I – nucleation rate (average results): slope of the tangent drawn on the high temperature side of the crystallization curve.

peak are associated to the type of nucleation mechanisms, to the nucleation and growth rates of the crystallites as well to their dimension and shape.[30] This crystallization process depends on the applied experimental conditions, such as time and temperature, and of the interactions between the blend materials.

The obtained results for the crystallization process are detailed in Table IV and shown in Figure 5.

An overall crystallization rate can be inferred from the difference between T_{co} and T_c.[20,53] A decrease of this temperature difference reveals an increase of the crystallization rate. This result shows that the binary blends have higher crystallization rates

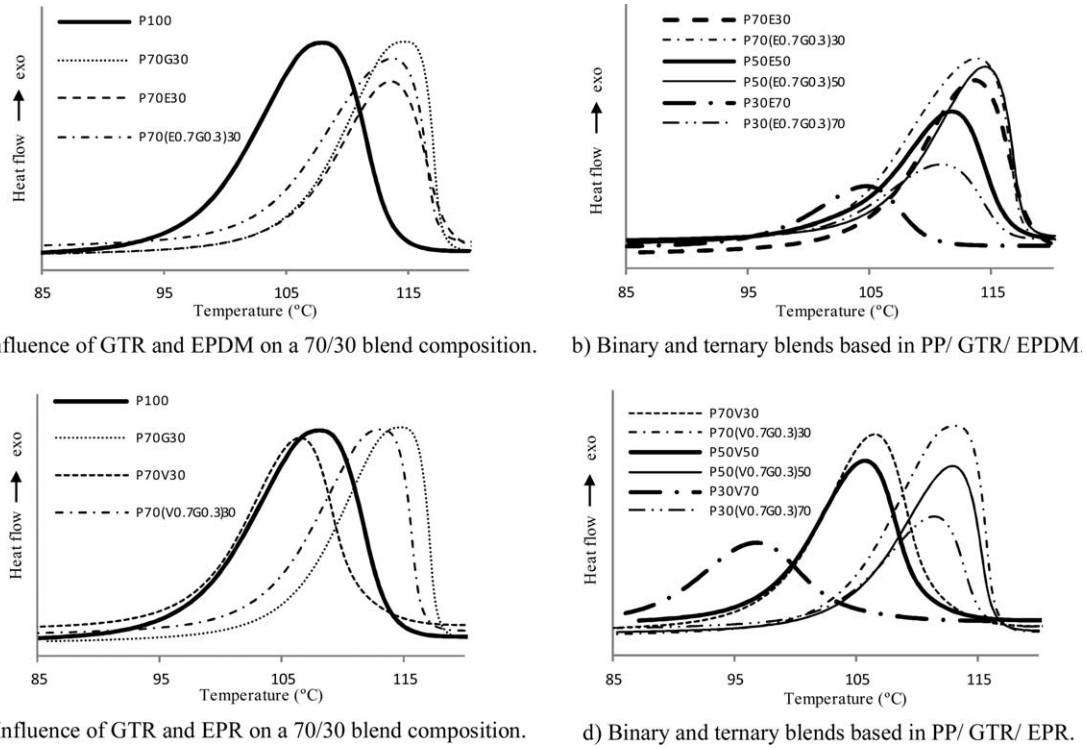

a) Influence of GTR and EPDM on a 70/30 blend composition. b) Binary and ternary blends based in PP/ GTR/ EPDM.

c) Influence of GTR and EPR on a 70/30 blend composition. d) Binary and ternary blends based in PP/ GTR/ EPR.

Figure 5. Crystallization peaks behavior obtained from DSC.

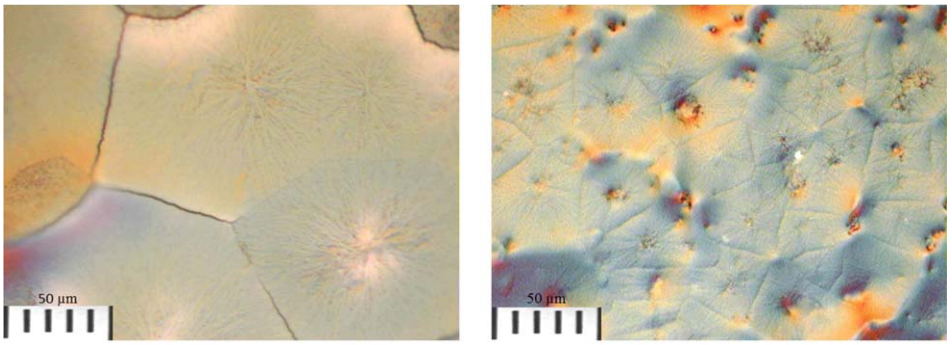

a) Reflection optical micrographs for sample PP (x50). b) Reflection optical micrographs for $P_{70}G_{30}$ blend (x50).

Figure 6. Microscopy analysis of PP and $P_{70}G_{30}$ blend. [Color figure can be viewed in the online issue, which is available at wileyonlinelibrary.com.]

than PP and that GTR presence induces the highest effect. The results indicate that $P_{70}G_{30}$ blend has also the highest nucleating rate, 137% higher than for PP. This GTR nucleating effect can be also identified in the TPE^{GTR} blends which reveal an increase on the nucleation rate. The ternary blends have similar T_{co} results, attributed to the higher nucleation effect of GTR.

A general increase of the T_{co} and T_c crystallization temperatures for the $P_{70}E_{30}$ and $P_{70}G_{30}$ binary blends and a small delay for the $P_{70}V_{30}$ blend is observed in Figure 5. The higher T_c results obtained for the EPDM and GTR binary blends reveal that both materials lead to the anticipation of the nucleation mechanism, by lowering the surface free energy barrier that hinders nucleation. These results indicate the existence of heterogeneous nucleation process within these blends.[42,54] On the EPR-based blends the shifting of T_c to lower temperatures can be explained by a dilution effect of the EPR amorphous component, being an indication of compatibility amongst the materials.[23,55] The higher affinity between PP and EPR with high propylene content (above 80%) can also lead to the existence of ethylene partially included in the inter-crystalline regions of the PP spherulites, reducing the crystal lamellae thickness and consequently lowering T_c. An increase of T_c with the EPDM presence shows this rubber nucleating effect in PP, by seeding the formation of crystallites structures at higher temperatures.[56–58]

As the rubber content increases a reduction on the nucleation rate and crystallization temperature is observed, which can be explained by an increasing restraining effect by EPR and EPDM on the mobility of the PP molecular chains.[23,26–28]

The effect of GTR particles on the crystallization process and on the increase of the TPE^{GTR} blend crystallinity can be explained by its strong nucleating effect and the almost simultaneous formation of nuclei, characteristic of heterogeneous nucleation mechanism.[43] A higher number of nuclei with similar growing rates will lead to a higher number of crystallites but with smaller dimensions, because of the occurrence of spherulite impingement at inferior crystallites radii. This nucleation and growing process leads to a finer microstructure and to smaller dimensional dispersion,[59] as seen in the melting peak width result ($T_{me} - T_{mo}$).

Microscopy Analysis. Microscopy analysis of PP sample and $P_{70}G_{30}$ blend, under reflection optical microscopy, is shown in Figure 6. Differences between the number and dimension of the crystallites, as well the impingement between them, are clearly seen in the micrographs. They clearly show the presence of a higher number of crystallites and with smaller dimensions in the $P_{70}G_{30}$ blend, confirming the GTR nucleating effect anticipated from the isothermal and nonisothermal studies.

Mechanical Properties. From previous works it is possible to establish some relationships between the crystallization process and the mechanical properties.[37,38] The TPE^{GTR} blends reveal a significant improvement in the impact resistance with EPR and EDPM, and a reduction of the tensile strength and Young modulus. It is well known that the crystallization process has a pronounced effect on the blends toughness. Failure can occur at the lamellae boundaries, being greater for larger size and perfection of the spherulites. The impact resistance is therefore strongly influenced by the resultant crystallinity and by the crystallites size and morphology.[32,60] Blends with lower crystallinity and with smaller and less perfect spherulites have an improved impact behavior. Lower blends crystallinity generally results on lower tensile stress and Young modulus, which explains the tensile strength patterns.

CONCLUSIONS

The crystallization study of TPE^{GTR} revealed a strong nucleation effect of GTR on the PP crystallization kinetics. EPDM shows to have a slight effect on the crystallization process, while EPR reveals no significant effect.

A predominantly heterogeneous nucleation mechanism on GTR-based blends is inferred from the isothermal and nonisothermal DSC analysis. A decrease of the half time of crystallization and increase on the rate constant k indicate a significant increase of the overall crystallization rate. The Avrami exponent n values ($\sim$3) confirm the heterogeneous mechanism and indicate a three-dimensional spherulitic growth. The nonisothermal curves of TPE^{GTR} blends reveal a higher crystallinity and prove the GTR effect on the PP crystallization behavior.

The different effects of EPDM and EPR in the GTR blend crystallization process can be explained by the EPR compatibility with PP.

An increase of the EPDM and EPR contents leads to a decrease of the crystallization temperature and nucleation rate, indicating that above certain contents the materials can be included within the PP spherulitic limits, constraining their nucleation and growth.

The TPE^{GTR} mechanical behavior can be explained and better understood on the basis of the crystallization process, more specifically from the resultant crystallinity and the dimension and structure of the crystallites.

A rheological study is being made to analyze and to improve the processing conditions of these TPE^{GTR} blends to obtain high added-value parts by injection molding technologies.

REFERENCES

1. Clauzade, C. Analyse du cycle de vie pour 9 voies de valorisation des pneus usages non reutilisables - document de réference. R&D Aliapur; Juin **2010**.
2. Fontaine, N.; Védrine, H. End of life vehicles. In: Council, E. P., Ed.; Directive 2000/53/CE. Official Journal of the European Union, Brussels, **2000**, p 18.
3. Guo, X.; Xiang, D.; Duan, G.; Mou, P. *Waste Manage.* **2010**, *30*, 4.
4. Isayev, A. I.; Yushanov, S. P.; Kim, S.-H.; Levin, V. Y. *Rheol. Acta* **1996**, *35*, 616.
5. Karger-Kocsis, J.; Mészaros, L.; Bárány, T. J. *Mater. Sci.* **2013**, *48*, 1.
6. Scuracchio, C. H.; Waki, D. A.; Bretas, R. S. *Polímeros: Ciẽncia e Tecnologia* **2006**, *16*, 46.
7. Zhang, X.; Lu, Z.; Tian, D.; Li, H.; Lu, C. *J. Appl. Polym. Sci.* **2013**, *127*, 4006.
8. Awang, M.; Ismail, H. *Polym. Test.* **2008**, *27*, 321.
9. Cossa, M. M.; Sirqueira, A. S.; Soares, B. G. *Polimeros* **2009**, *19*, 190.
10. Grigoryeva, O.; Fainleb, A.; Shumskii, V.; Vilenskii, V.; Kozak, N.; Babkina, N. *Polym. Sci. Ser. A* **2009**, *51*, 216.
11. Ismail, H.; Awang, M.; Hazizan, M. A. *Polym. Plast. Technol. Eng.* **2006**, *45*, 463.
12. Kumar, C. R.; Fuhrmann, I.; Karger-Kocsis, J. *J. Polym. Degrad. Stab.* **2002**, *76*, 137.
13. Lievana, E.; Karger-Kocsis, J. Progress in rubber. *Plast. Recyd. Technol.* **2004**, *20*, 1.
14. Qin, J.; Ding, H.; Wang, X.; Xie, M.; Yu, Z. *Polym. Plast. Technol. Eng.* **2008**, *47*, 199.
15. Wiessner, S.; Wagenknecht, U.; Zichner, M.; Michael, H.; Heinrich, G. *Plast. Rubber Compos.* **2006**, *35*, 393.
16. Zhang, S. L.; Zhang, Z. X.; Xin, Z. X.; Pal, K.; Kim, J. K. *Mater. Des.* **2010**, *31*, 1900.
17. Zhang, X.; Lu, C.; Liang, M. *J. Appl. Polym. Sci.* **2011**, *122*, 2110.
18. Lei, Y.-G.; Chan, C.-M.; Wang, Y.; Ng, K.-M.; Jiang, Y.; Lin, L. *Polymer* **2003**, *44*, 4673.
19. Mucha, M.; Królikowski, Z. *J. Therm. Anal. Calorim.* **2003**, *74*, 549.
20. Chen, J.; Cao, Y.; Li, H. *J. Appl. Polym. Sci.* **2009**, *116*, 1172.
21. Groeninckx, G.; Vanneste, M.; Everaert, V. Crystallization, morphological structure, and melting of polymer blends. In: Polymer Blends Handbook; Utracki, L. A., Ed.; Kluwer Academic: Dordrecht, **2003**; p 203.
22. Lopez Manchado, M. A.; Biagiotti, J.; Torre, L.; Kenny, J. M. *J. Therm. Anal. Calorim.* **2000**, *61*, 437.
23. Yokoyama, Y.; Ricco, T. *J. Appl. Polym. Sci.* **1997**, *66*, 1007.
24. Van der Wal, A.; Mulder, J. J.; Oderkerk, J.; Gaymans, R. J. *Polymer* **1998**, *39*, 6781.
25. Stelescu, M.; Airinei, A.; Grigoras, C.; Niculescu-Aron, I. -G. *Int. J. Thermophys.* **2010**, *31*, 2264.
26. Martuscelli, E.; Silvestre, C.; Abate, G. *Polymer* **1982**, *23*, 229.
27. Greco, R.; Mancarella, C.; Martuscelli, E.; Ragosta, G.; Jinghua, Y. *Polymer* **1987**, *28*, 1929.
28. D'Orazio, L.; Mancarella, C.; Martuscelli, E.; Sticotti, G.; Ghisellini, R. *J. Appl. Polym. Sci.* **1994**, *53*, 387.
29. Da Silva, A. L. N.; Rocha, M. C. G.; Lopes, L.; Chagas, B. S.; Coutinho, F. M. B. *J. Appl. Polym. Sci.* **2001**, *81*, 3530.
30. Choudhary, V.; Varma, H. S.; Varma, I. K. *Polymer* **1991**, *32*, 2534.
31. Brostow, W.; D'Souza, N. A.; Galina, H.; Ramamurthy, A. C. *Polym. Eng. Sci.* **1996**, *36*, 1101.
32. Perkins, W. G. *Polym. Eng. Sci.* **1999**, *39*, 2445.
33. Costa, H. M.; Ramos, V. D.; Rocha, M. C. G. *Polym. Test.* **2006**, *25*, 498.
34. Wiessner, S. W. U.; Zichner, M.; Michael, H.; Heinrich, G. Effects of interface reactions in compatibilised rubber powder-polypropylene–TPEs. Polymer Processing Society: Leipzig, **2005**.
35. Silva, L. P.; Rocha, J. S.; Pacheco, E. B. V.; Bouças, T. A. O.; Furtado, C. R. G. *Int. J. Polym. Mater.* **2008**, *57*, 555.
36. Costa, H. M.; Ramos, V. D. *Polym. Test.* **2008**, *27*, 27.
37. Lima, P. S.; Oliveira, J. M.; Costa, V. A. F. *J. Appl. Polym. Sci.* **2015**, *132*, 42011.
38. Lima, P. S.; Oliveira, J. M.; Costa, V. A. F. *J. Appl. Polym. Sci.* **2014**, *131*, 40160.
39. Gottfried, W.; Ehrenstein, G. R.; Pia, T. Thermal Analysis of Plastics: Theory and Pratice; Hanser Gardner Publications: München, **2004**.
40. Avrami, M. *J. Chem. Phys.* **1939**, *7*, 1103.
41. Jang, G.-S.; Jo, N.-J.; Cho, W.-J.; Ha, C.-S. *J. Appl. Polym. Sci.* **2002**, *83*, 201.
42. Massa, M. V.; Carvalho, J. L.; Dalnoki-Veressa, K. *Eur. Phys. J. E Soft Matter* **2003**, *12*, 111.
43. Seo, Y.; Kim, J.; Kim, K. U.; Kim, Y. C. *Polymer* **2000**, *41*, 2639.
44. Srinivas, S.; Babu, J. R.; Riffle, J. S.; Wilkes, G. L. *Polym. Eng. Sci.* **1997**, *37*, 497.
45. Kang, J.; Li, J.; Chen, S.; Peng, H.; Wang, B.; Cao, Y.; Li, H.; Chen, J.; Gai, J.; Yang, F.; Xiang, M. *J. Appl. Polym. Sci.* **2013**, *129*, 2663.

46. Ehrenstein, W. G.; Riedel, G.; Trawiel, P. Thermal Analysis of Plastics; Hanser Publishers: Munich, **2004**.
47. Mandelkern, L. Crystallization of Polymers: Kinetics and Mechanisms; Cambridge University Press: Cambridge, **2004**.
48. Naffakh, M.; Martín, Z.; Marco, C.; Gómez, M. A.; Jiménez, I. *Thermochim. Acta* **2008**, *472*, 11.
49. Zhang, Y.-F.; Xin, Z. *J. Polym. Sci. Part B: Polym. Phys.* **2007**, *45*, 590.
50. Cho, K.; Li, F.; Choi, J. *Polymer* **1999**, *40*, 1719.
51. Zysk, T.; Zhao, S. G.; Ehrenstein, G. W. *Kautsch Gummi Kunstst.* **1992**, *45*, 943.
52. Grigoryeva, O.; Fainleib, A.; Tolstov, A.; Pissis, P.; Spanoudaki, A.; Vatalis, A.; Delides, C. *J. Therm. Anal. Calorim.* **2006**, *86*, 229.
53. Choudhary, V.; Varma, H. S.; Varma, I. K. *J. Therm. Anal.* **1987**, *32*, 579.
54. Martuscelli, E. *Polym. Eng. Sci.* **1984**, *24*, 563.
55. Li, Y.; Xu, J.-T.; Dong, Q.; Wang, X.-P.; Fu, Z.-S.; Fan, Z.-Q. *Polym. Plast. Technol. Eng.* **2008**, *47*, 1242.
56. Martuscelli, E.; Silvestre, C.; Bianchi, L. *Polymer* **1983**, *24*, 1458.
57. Silva, A. L. N.; Tavares, M. I. B.; Politano, D. P.; Coutinho, F. M. B.; Rocha, M. C. G. *J. Appl. Polym. Sci.* **1997**, *66*, 2005.
58. Wenig, W.; Asresahegn, M. *Polym. Eng. Sci.* **1993**, *33*, 877.
59. Purnima, D.; Maiti, S. N.; Gupta, A. K. *J. Appl. Polym. Sci.* **2006**, *102*, 5528.
60. Wang, K.; Wu, J.; Ye, L.; Zeng, H. *Compos. Part A-Appl. Sci. Manuf.* **2003**, *34*, 1199.